Series: Optoelectronic Materials and Devices

Volume 1

Non-Crystalline Materials for Optoelectronics

INOE
2004

Series: Optoelectronic Materials and Devices

Volume 1

Non-Crystalline Materials for Optoelectronics

Editors:

G. Lucovsky
North-Caroline State University
Raleigh, USA

M. Popescu
National Institute of Materials Physics
Bucharest, Romania

INOE
2004

CONTENTS

Chapter 2

Photo-structural transformations and global connectedness of network glasses

Fei Wang, P. Boolchand

Department of Electrical, Computer Engineering and Computer Science
University of Cincinnati, Cincinnati, Ohio 45221-0030, USA

Illumination of chalcogenide glasses and amorphous thin-films by near band-gap radiation produces charge carriers that recombine producing local structural rearrangements including switching of covalent bonds. Under increased illumination, such rearrangements can propagate globally in networks that are stress-free (*intermediate phases)* dynamically transforming a *self-organized state* (*intermediate phases*) into a light-soaked *random network state,* and leading to pronounced photo-diffusion, photo-expansion and eventually photo-melting. On the other hand, in stress-prone networks (*floppy* and *stressed-rigid* phases) structural rearrangements are largely localized where light is absorbed. In the latter phases, networks are usually found to be *de-mixed* on a nanoscale, and photo-polymerization effects abound as free internal surfaces reconstruct. Raman- and Brillouin-scattering observations bearing on these results are reviewed.

Light induced effects in chalcogenide glasses

Overview

Light induced effects in chalcogenide glasses and thin-films have displayed a richness of phenomenology that has attracted widespread interest for over three decades. Some of these effects include photo-darkening [1], photo-fluidity [2], giant-photodensification [3], photochemical dissolution [4], anisotropic opto-mechanical response [5], photocrystallization [6] and phase change [7]. These effects have stimulated applications and some of these include phase-change memories, programmable metallization cell memories [8], digital video discs [9], xerography [10], and x-ray imaging [11] to mention a few.

Two general themes have evolved in understanding the richness of these phenomena. One has emphasized the electronic origin of these effects [12-14], and

Series: Optoelectronic Materials and Devices, ISSN 1584-5508
Volume 1, 2004, Non-Crystalline Materials for Optoelectronics, ISBN 973-85818-0-X

metastability of local structures formed as charge carriers are produced (by pair-producing radiation) and eventually recombine. The second theme has emphasized aspects of global structure, mainly layered structures [15] (in the stoichiometric As_2Se_3 and As_2S_3 glasses), to understand evolution of photo-darkening and other photo-effects.

Role of network connectedness

Currently, little is known on how global connectivity of a disordered network influences the manner in which pair-producing radiation interacts with it. In this work, we describe recent experiments that underscore the close connections between light-induced effects and the connectivity as measured by mean-coordination number (r) of a disordered network. Network glasses can be broadly classified [16-18] according to their elastic response into *floppy, intermediate and stressed-rigid* atomic structures. *Floppy* and *Stressed-rigid* glass compositions generally form backbones that are *stress-prone*, in sharp contrast to *Intermediate phase* glass compositions that possess backbones that are not only *stress-free* but also that character does not change with time i.e., *age* [19-21]. For the readers benefit we introduce the ideas that have led to this structure based classification of glasses in the next section. *Intermediate Phase* glass compositions when subjected to increasing flux of pair-producing radiation exhibit photo-structural transformations; the pristine *self-organized state* transforms into a light- soaked *random network* state. Two examples of systems [22,23] where such effects are observed will be described latter.

Floppy and Stressed-rigid glass compositions differ from *Intermediate Phase* glass compositions in several other somewhat subtle respects. *Real glasses, in these phases* are usually *demixed* on a nanoscale [24-27] into molecular clusters although exceptions can occur. For example, bulk alloy As_xS_{1-x} glasses in S-rich regime ($x < 0.25$) and S-deficient one ($x > 0.40$) are known to possess respectively S_8 crowns, and As_4S_4 and As_4S_3 monomers. Such segregation can become pronounced in vapor-deposited thin-films. When illuminated by band-gap radiation, backbones of *bulk glasses* usually photo-polymerize reversibly as concentrations of monomeric species systematically decrease with increasing light-flux. The process briefly consists of band-gap light serving to reconstruct internal surfaces of fragmented networks to qualitatively change their morphology and polymerize them. Several examples illustrating these effects will be presented towards the end of the chapter. We conclude by providing a brief summary of the principal results.

Three elastic phases of network glasses

Mean-field rigidity transition in disordered networks

J.C. Phillips was one of the first to formalize [28] the importance of global connectivity in describing the physical properties of glasses in terms of constraint theory. Lagrangian constraints due to near-neighbor valence forces (bond-stretching and bond-bending) are usually intact while those due to more distant neighbors broken as glass forming melts are cooled to form bulk glasses. The

essence of *constraint theory* is the recognition that highly over-connected ($r > 3$) or under-connected ($r < 2$) networks do not form glasses, but optimally constrained ones ($r \sim 2.4$) readily do. Here r represents the mean coordination number; and the magic value of $r = 2.4$ corresponds to the circumstance when the count of Langrangian constraints per atom $n_c = 3$, the three degrees of freedom per atom in a 3d network. M. F. Thorpe recognized [29] that when the mean-coordination number of a covalently bonded *random* network increases to $r = 2.40$, the network undergoes a phase transition from an elastically floppy to a stressed-rigid state. This is the Phillips-Thorpe rigidity transition [30]. The floppy to rigid phase transition in a *random* network near $r = 2.4$ also coincides with optimization of the glass-forming tendency.

Two elastic phase transitions observed in self-organized networks

In 1999, it emerged that there are, in fact, *two* rigidity transitions and not *one* as predicted by mean-field theory. Using Raman scattering and T-modulated Differential Scanning Calorimetry, Selvanathan et al.[31] showed the existence of two distinct elastic phase transitions in binary Si_xSe_{1-x} glasses. Similar results have been seen in other binary (P_xSe_{1-x} [27], As_xSe_{1-x} [32], Ge_xSe_{1-x} [22,33]) and ternary ($As_xGe_xSe_{1-2x}$ [34], $P_xGe_xSe_{1-2x}$ [21,35]) chalcogenide glasses, thus, underscoring the generality of the result. Examination of several glass systems has shown that the *solitary* rigidity transition (predicted by mean-field constraint theory) is the exception. The usual behavior consists of opening of *intermediate phases* between *floppy* and *stressed-rigid* ones as schematically illustrated in Fig. 1. Numerical simulations [18,36] suggest that these phases can form over a range of global connectivities near the mean-field rigidity transition. The network backbone consists of local- and medium-range structures that are *isostatically rigid*, i.e., rigid but stress-free, and is described as *self-organized*.

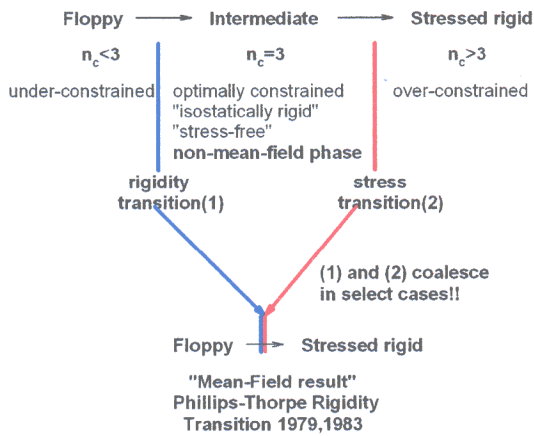

Fig. 1. Intermediate phases bounded by rigidity- (blue) and stress-(red) transition open between floppy and stressed rigid elastic phases in real glasses. In random networks the two transitions coincide and one expects a solitary rigidity transition as predicted by mean-field theory.

How does one recognize whether a glass composition belongs to an intermediate phase? Examination of glass transitions (T_g) using T-modulated DSC (MDSC) has made it possible to separate the *reversing enthalpy* from the *non-reversing enthalpy* (ΔH_{nr}) associated with T_g as discussed elsewhere [19,32,37]. The latter endotherm is a signature of *ergodicity breaking events* when structural arrest of a glass forming liquid occurs near T_g. For glass compositions that reside in intermediate phases the ΔH_{nr} term is found to nearly vanish. Experiments on several families of glasses [21, 31-34] have shown that the endotherm (ΔH_{nr}) has a square-well like variation with walls near $r_c(1)$ and $r_c(2)$, and the glass transition becomes thermally reversing in the $r_c(1)<r<r_c(2)$ range (thermally reversing window) Raman – active mode of select local structures in the backbone, is found to display vibrational frequencies (ν_{cs}) that show a power-law dependence on $r-r_c$. One such mode in question is the strongly active symmetric breathing mode of corner-sharing tetrahedral units ($GeSe_4$ as for example). One observes distinct elastic power-laws in the composition regimes $r_c(1) < r < r_c(2)$ (*the window*), and above (*the window*) $r > r_c(2)$. Thus $r_c(1)$ and $r_c(2)$ not only represent the onset and end of *reversibility windows* from thermal measurements, but also the rigidity-($r_c(1)$) and stress- ($r_c(2)$) transition phase boundaries in Raman optical elasticities [20,34,35]. Theoretical justification for these elastic phases has emerged from numerical simulations on self-organized networks as described [18,36] elsewhere.

Intermediate phases are special

Network backbones for glass compositions in *intermediate phases* display rather exceptional mechanical, thermal and optical properties. The atomic scale organization of a network backbone that leads to this unusual physical behavior is also quite special. These glass compositions usually form space filling networks displaying the smallest molar volumes [38]. At a local structural level, network building blocks possess a count of Lagrangian constraints/atom (n_c) due to bond-stretching and bond-bending forces of 3. Such units are rigid but stress-free, i.e., isostatically rigid [39] and their presence lowers free energy of backbones. At a medium-range structural level, rigidity is traced to rings of specific size. In 3 dimensional networks, rings possessing 6 atoms represent the marginal case [39], i.e., larger-sized rings ($n > 6$) are floppy while smaller-sized ones ($n < 6$) are stressed-rigid. Population of such local and medium range structures lowers the free energy of intermediate phases.

Intermediate phases have now been observed in several glass systems. Fig. 2 provides an overview of results in which the range of mean-coordination number r spanned by these phases is shown in red. In multi-component chalcogenide glasses containing equal fractions of group III and V elements, in general, intermediate phases span a wide range of mean-coordination number r. On the other hand, in chalcohalide glasses these phases occur over a much narrower range of r for reasons discussed ahead.

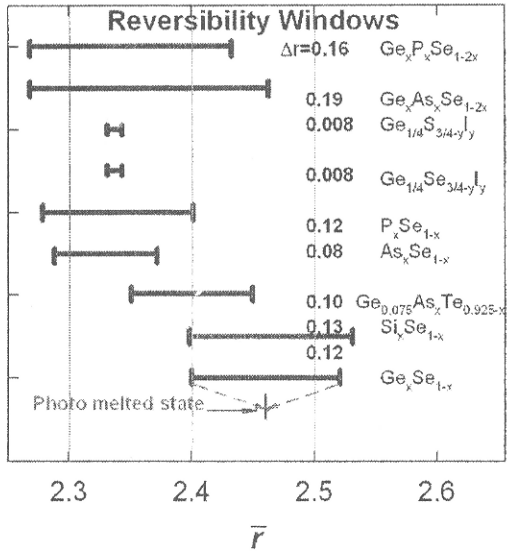

Fig. 2. Trends in intermediate phases observed in indicated chalcogenide and chalcohalide glasses taken from refs.21,22,27,32-35.

The large width of intermediate phases in chalcogenides glasses is related [21, 34, 37] to the fact that there are *several* As-centered (r = 2.28, 2.40) and Ge-centered (r = 2.40, 2.67) isostatic local units that form building blocks of their backbones and together these local units span a range of r contributing to widths of intermediate phases. The sharp reduction in widths of these phases in the two chalcohalide glass systems in Fig. 2 comes from replacement of bridging selenium (sulfur) sites in the backbone by one-fold coordinated iodine sites *randomly* [23,37]. The replacement of iodine by Se rapidly narrows the range of r wherein isostatic rigidity can be nucleated. In these chalcohalides there is only one isostatic local structure populated [40] as we shall see later. The sharp reduction of T_g in the two chalcohalide glasses as a function of increasing iodine for sulfur or selenium replacement is in excellent accord with the molecular structure of these glasses probed in Raman scattering [40]. Furthermore, these observations are in harmony with the interpretation of glass transition temperature as a measure of network connectedness as suggested from *stochastic agglomeration theory* developed by R. Kerner and M. Micoulaut [41,42].

Photo-structural transformations and intermediate phases

The unusual response of intermediate phases to illumination by near band-gap radiation was first noted in Raman scattering measurements performed as a function of laser illumination power. In this section we describe results on a prototypical chalcogenide and chalcohalide glass system that highlight the underlying photo-structural transformations.

Chalcogenide glasses: Ge_xSe_{1-x}

Two types of Raman scattering setups were used to carry forward these experiments [22,33] on the binary Ge-Se glass system. A conventional (macro-Raman) setup wherein typically the laser beam is bought [22] to a loose focus (50 μm spot size) and a micro-Raman set-up [33] in which the exciting laser beam is bought to a tight focus (1 μm spot size) using a microscope attachment. In both set of experiments about a mW of 647 nm radiation from a Kr^+ ion laser was used. In the macro-configuration the laser beam flux is low (10^{-3} mW/ μm^2), and one observes [22] the intrinsic elastic phases of glasses described earlier. These phases include a *floppy* phase at $x < 0.20$, an *intermediate* phase extending in the $0.20 < x < 0.25$ range, and the *stressed-rigid* phase at $x > 0.26$. Compositional trends in the frequency of the corner-sharing $Ge(Se_{1/2})_4$ tetrahedra (shown in Figs. 3a) reveal an elastic power-law in the *stressed-rigid* phase at $x > 0.26$ with a value of $p = 1.54(10)$ that is in excellent agreement with numerical predictions [43,44].

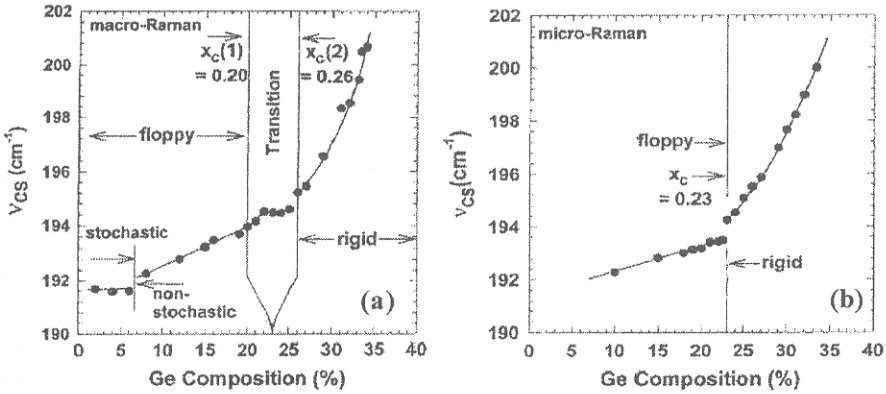

Fig. 3. (a) Variations in frequency of CS mode, $\nu_{CS}(x)$, of $Ge(Se_{1/2})_4$ tetrahedra in (a) macro-Raman and (b) micro-Raman experiments on Ge_xSe_{1-x} glasses revealing presence of the intermediate phase ($0.20 < x < 0.25$) in the former and its collapse in the latter experiments. The collapse is thought to be a photostructural effect leading to light-induced melting of the intermediate phase. See ref.22.

In the micro-Raman configuration the laser beam flux (1mW/ μm^2) is nearly three orders of magnitude higher than in the macro-Raman one, with the consequence that one observes the light-modified state of these elastic phases. The *intermediate phase* is found to collapse at its centroid (near $x = 0.23$) (Fig. 3b), and the *stressed-rigid* phase commences at $x > 0.23$ already. In the micro-Raman measurements, near band-gap radiation produces electron-hole pairs leading to formation of metastable local defect configurations that serve to mediate rapid switching of normal covalent bonds [12]. The first step of light soaking is photo-diffusion and with increasing light flux, the final step consists of a *random network*

which replaces the virgin *self-organized* state. The virgin- and light-soaked-state represent respectively the two extremes [18, 29] of rigidity onset in network glasses predicted by theoretical simulations (Fig. 1), one giving rise to the *presence* of an *intermediate phase* when a network *self-organizes*, and the other to absence of it when a network acquires a *random* atomic structure.

Chalcohalide glasses: $Ge_{1/4}Se_{3/4-y}I_y$

The *intermediate phase* in binary Ge-Se glasses [22] is narrowed dramatically by chemically alloying iodine [23]. This was revealed by examining ternary $Ge_{1/4}Se_{3/4-y}I_y$ glasses in Raman scattering and MDSC experiments systematically as a function of y. A count of Lagrangian constraints in the present ternary shows that the elastic phase boundary between *stressed rigid* ($y < y_c$) and *floppy* ($y > y_c$) glasses occurs at $y_c = 1/6$ [45]. Taking the coordination number of Ge, Se and I to be respectively as 4, 2 and 1, one obtains the mean coordination number of the ternary glass as,

$$r = 4(1/4) + 2(¾ - y) + y \qquad (1)$$

For a glass network containing a n_l/N fraction of dangling ends (iodine atoms) to be optimally connected, one requires [46]

$$r = 2.4 - 0.4\,(n_l/N) \qquad (2a)$$

or $$1 + 1.5 - y = 2.4 - 0.4y$$

or $$y = y_c = 1/6 \qquad (2b)$$

In Raman scattering experiments performed at low power (1mW), one observes modes of mixed $Ge(Se_{1/2})_{4-m}I_m$ tetrahedral units with m = 1, 2 , 3 and 4 iodine near-neighbors. As the concentration of iodine in the alloys is increased, the m = 1 units grow at the expense of m = 0 units as shown in Fig. 4. Of special note is the step in the concentration of m = 1 units (N_1/N) in the $y_1 = 0.155 < y < y_2 = 0.164$ range. The m = 1 units are rather special. A count of Lagrangian constraints per atom shows [37, 47] such units to be isostatically rigid ($n_c = 3$).

MDSC experiments on these ternary glasses have independently served to confirm the *intermediate* phase through a measurement of the non-reversing enthalpy near T_g [23]. The enthalpy term displays a minimum in the same $0.155 < y < 0.164$ iodine concentration range as illustrated in Fig 5. For the reader's convenience, we have included in Fig. 5, a plot of the concentration of m = 1 units from the Raman scattering results. We note that the linear step in N_1/N coincides with walls of the thermally reversing window, and both sets of measurements independently reinforce the notion that the intermediate phase extends in the $0.155 < y < 0.164$ iodine concentration range. The sharp linear increase in concentration of the m = 1 units (N_1/N) at the expense of the m = 0 units in the intermediate phase is an intriguing result. The m = 1 units are isostatically rigid structures while the m = 0 units stressed-rigid ones. The sharp increase in N_1/N in the narrow

thermally reversing window can thus be viewed as a structural reorganization that serves to minimize backbone stress, and represents a feature of self-organization in the ternary.

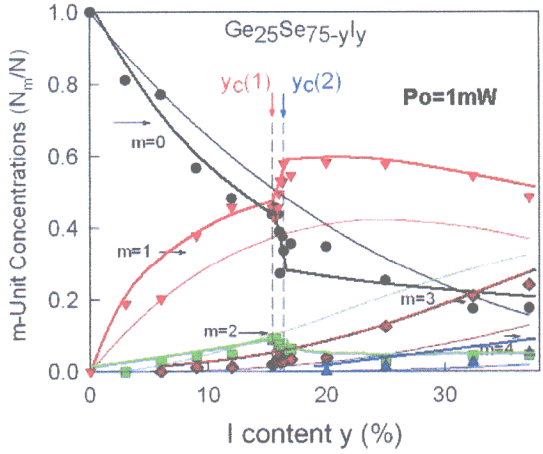

Fig. 4. Variations in the concentration of pure and mixed $Ge(Se_{1/2})_{4-m}I_m$ units as a function of iodine concentration, y, deduced from deconvolution of Raman lineshapes studied at Po = 1 mW of 647 nm radiation. The thin-lines give prediction of m-unit concentrations based on combinatorics (ref. 45). The thick-lines give present experimental results. In the macro-Raman setup the exciting beam is brought to a loose focus and penetrates through the bulk of the sample contained in a quartz tube. Thermal effects in such a setup are expected to be minimal. Fig is taken from ref. 23.

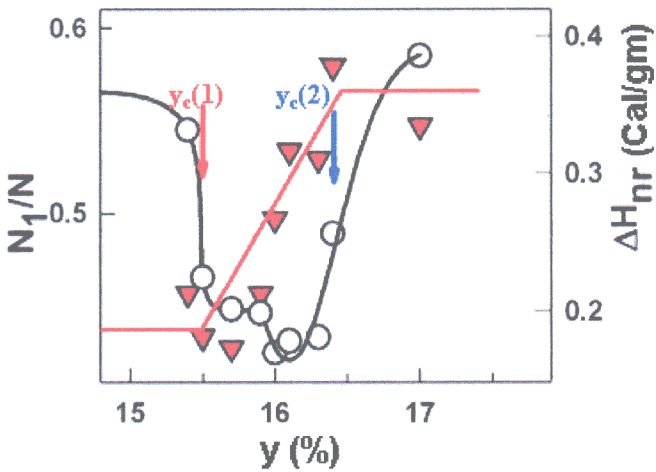

Fig. 5. Variations in non-reversing enthalpy $\Delta H_{nr}(y)$ near T_g (open circles) and concentration of m = 1 units, N_1/N (y) (red triangles), illustrating the onset (y_c (1) = 0.155, red arrow) and end ($y_c(2)$ = 0.164, blue arrow) of the intermediate phase in the $Ge_{25}Se_{75-y}I_y$ ternary.

The influence of increasing laser excitation power, Po, in the 1 mW < Po < 15 mW range has also been examined, and the results appear in Figs. 6 and 7. Upon increasing the power Po to 15 mW the N_1/N -step vanishes as shown in Fig. 6. The essential changes in Raman lineshapes as a function of Po are included in Fig. 7 and include a reduction in the N_1/N step height as Po increases. The intermediate phase in $Ge_{1/4}Se_{3/4-y}I_y$ glasses observed at low Po (=1 mW) apparently transforms into a random network state as laser power increases to Po = 15 mW. These observations are parallel to those encountered earlier on the Ge-Se binary [22] in Fig. 4 and 5. In both cases, the *self-organized state* of glasses prevailing at low Po is transformed as the illuminating power Po is increased. The sub-bandgap radiation penetrates deep in the samples and one expects the observed changes to be bulk and not surface effects. In these macro- Raman scattering measurements the excitation radiation serves as a *pump* to effect photo-structural transformations as well as a *probe* of the ensuing structural changes of the backbone. An attractive aspect of these measurements is that the transformed sample volume along the laser beam (several mm thick bulk glass sample contained in a quartz tube) is also the region that gives the Raman signal.

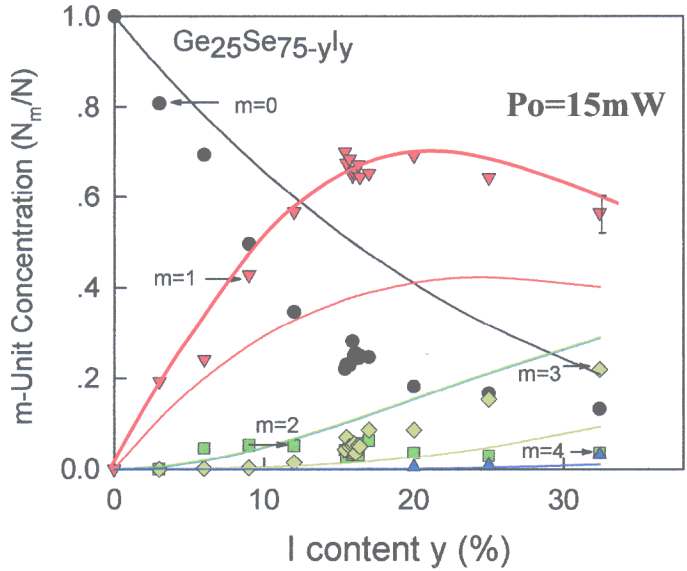

Fig. 6. Variations in concentrations of various m-units examined in Raman scattering at Po = 15 mW. The thin colored lines give the predicted variation of N_m/N units based on combinatorics (ref. 45). Experimental conditions are similar to those used in Fig. 4 and thermal effects are expected to be minimal.

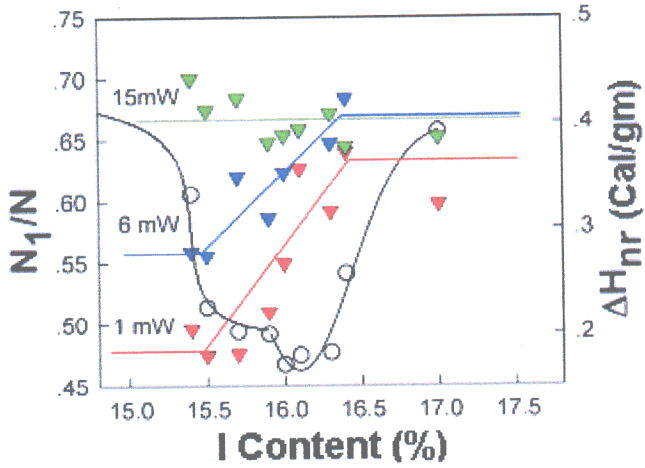

Fig. 7. Variation in concentration of m = 1 units in $Ge_{1/4}Se_{3/4-y}I_y$ glasses deduced from Raman scattering as a function of indicated laser excitation power Po. The N_1/N step height reduction with increasing power constitutes evidence for photo- melting of the intermediate phase in the $0.155 < y < 0.164$ range. See ref. 23 for details.

These light-induced structural transformations observed in *intermediate phases* of a chalcogenide and a chalcohalide glass serves to demonstrate the commonality of the underlying effects. In both cases the backbones in the pristine state are viewed to be *self-organized*. The absence of global stress in *intermediate phases* apparently facilitates underlying photostructural transformations. In both cases the interaction of band-gap light produces electron- hole pairs that produce metastable defects that lead eventually to switching of covalent bonds as carriers recombine. The switched covalent bond configuration leads to photodiffusion as described earlier by H. Fritzsche [12]. With increasing illumination power photodiffusion gives way to photomelting as more optical energy is pumped per unit time in the virgin *self-organized state* to completely transform it to a light-soaked *random network state*. The later state can be viewed as an excited state of the backbone. And upon lowering illumination power one recovers the virgin *self-organized state* showing that the underlying athermal transformation is *reversible* in nature.

Intermediate phases and absence of network stress

Stress in disordered networks is a challenging subject because several inter related factors contribute to it. Some of these factors include (i) atomic size- and (ii) atomic mass- distributions, and (iii) network connectivity on a local and global scale. Strain and rigidity in disordered networks are concepts that have connections

to both elements of local- and global- structure. Although numerical simulations [18,36] and constraint counting algorithms suggest glasses in intermediate phases possess stress-free backbones, currently, there is no direct experimental evidence for such a behavior. We have recently carried forward Raman pressure experiments that provide the first clues to decode aspects of network stress in glasses. The system of choice is the Ge-Se binary; in this system atomic masses and sizes are nearly the same, and furthermore, intermediate phase glass compositions are well established. Raman scattering is the method of choice to probe these effects because it permits examining glasses at all length scales.

Raman pressure measurements on Ge-Se glasses

The influence of hydrostatic pressure on Raman scattering from crystalline chalcogenides, such as As_2S_3 and P_4S_3 has been examined [48, 49] in considerable detail in the past. A larger blue-shift of inter-planar or inter-cluster modes is observed in contrast to intra-layer or intra-cluster ones reflecting the weaker strength of van der Waals forces in relation to covalent forces. Very few such measurements have been made on glassy chalcogenides. An important difference between the response of ordered networks (crystals) from disordered ones (glasses) is the existence of a threshold behavior in the pressure-induced shifts of vibrational modes in the latter systems, particularly when atom-size and -mass distributions are nearly the same. Raman pressure measurements on $GeSe_2$ glass by K. Murase and T. Fukunaga [50, 51] have shown that the symmetric stretch mode frequency of $Ge(Se_{1/2})_4$ tetrahedra does not blue-shift until the applied pressure exceeds a threshold value; $P = P_c = 35$ kbar. The threshold P_c provides then a measure of internal stress of the backbone.

We have carried out Raman scattering measurements as a function of hydrostatic pressure over a wide range of network connectedness in binary Ge_xSe_{1-x} glasses. These measurements utilized a Diamond Anvil Cell with alcohol methanol mixture as a pressure transmitting medium, and a micro-Raman set up with a BX 41 Olympus microscope attachment. The pressure was calibrated using Ruby fluorescence and the hydrostatic nature of the pressure confirmed by fluorescence lineshapes. Fig. 8 displays the pressure induced shift in vibrational mode frequency (ν_{CS}) of corner-sharing $Ge(Se_{1/2})_4$ terahedra. These units are of interest because they form part of the backbone in these binary glasses. With increasing x, rigidity first percolates at the rigidity transition ($x_c(1) = 0.20$), and with a further increase of x, stress onsets at the stress-transition ($x_c(2) = 0.25$) as noted earlier [22, 23] from MDSC and ambient pressure Raman measurements. The results on the present glasses reveal rather interesting trends in P_c (Fig. 8a and b). One observes the mode frequency $\nu_{CS}(P)$ to blue-shift as a function of external pressure but only once $P > P_c$.

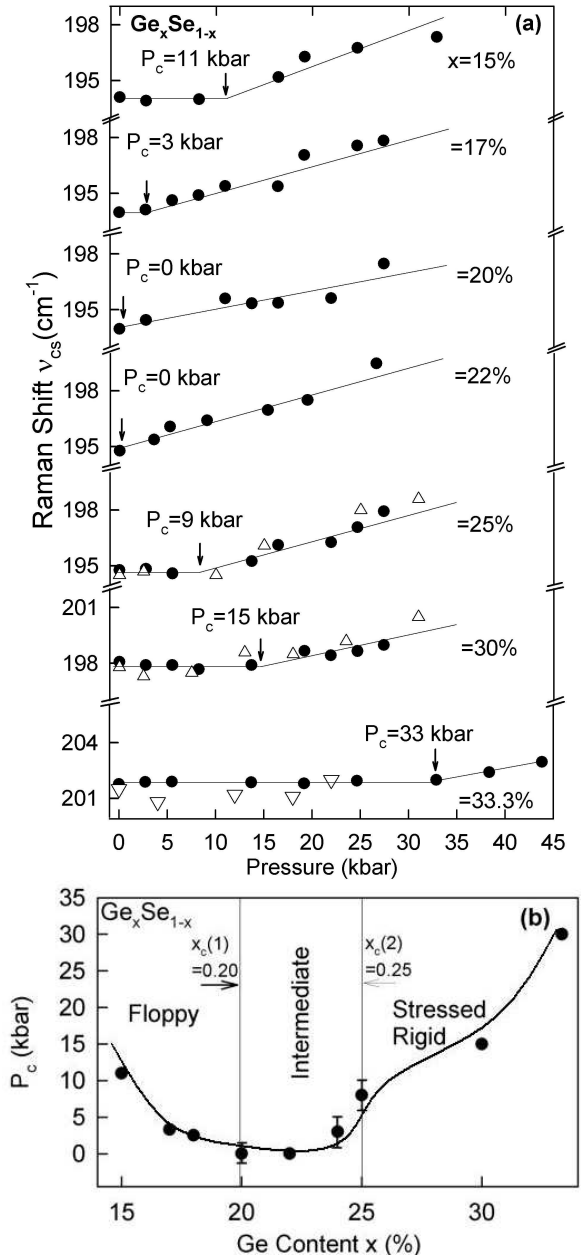

Fig. 8.(a) Variations in mode frequency of CS $Ge(Se_{1/2})_4$ units studied as a function of external pressure P in binary Ge_xSe_{1-x} glasses at different Ge concentrations x expressed in %. Note the existence of a threshold pressure P_c above which the mode blue-shifts. The (Δ) points are taken from ref. 50 while the (•) points are from present work, (b) Trends in $P_c(x)$ show the existence of a window that coincides with the intermediate phase glass compositions.

Note that P-induced changes in ν_{CS} first occur near 33 kbars in the *stressed rigid* stoichiometric $GeSe_2$ glass, but already near 0 kbar for glasses at x = 20 at.% and 22 at.% of Ge. Variations in threshold pressures P_c display a rather interesting trend: P_c steadily increases at $x > x_c(2)$ or at $x < x_c(1)$ but almost vanishes in the $x_c(1) < x < x_c(2)$ composition range, the *intermediate phase*. The most natural interpretation of these trends is that P_c provides a measure of intrinsic network stress of the backbone, and that it nearly vanishes in the *intermediate phase* but reappears both in the *stressed-rigid* and *floppy* phases of the present binary glass system. The backbones of glasses become increasingly stressed at $x > 0.25$ as network global connectivity progressively increases in the *stressed-rigid* phase. This is the expected behavior. However, the present results also demonstrate that backbones of glasses at $x < 0.20$ are increasingly also stressed as they get floppier, a result that is intriguing to say the least. A possible interpretation could be that presence of floppy or bond-rotation modes serves to locally stress backbones due to the strongly repulsive van der Waals forces that keep Se chains apart as reflected in the steadily increasing molar volumes [38] as the chain-fraction increases when x approaches 0.

Giant photo-elastic response of Ge-Se glasses in Brillouin scattering

The role of network connectedness in light-induced effects in glasses has emerged in an elegant fashion from recent Brillouin scattering (BS) measurements [52]. BS serves as a complementary vibrational spectroscopy to Raman scattering in glasses. Raman scattering permits probing optical excitations, while Brillouin scattering permits accessing acoustic excitations in solids. Relaxation of the k = 0 selection rule in glasses permits vibrational modes of local units such as tetrahedra or pyramids to be observed in Raman scattering. Furthermore, variations in frequency of these local units examined systematically as a function of mean-coordination number, ***r***, has served to probe the global elastic phases [22,23] of network glasses. Thus, Raman scattering permits probing disordered networks both at a *local* and also at an *extended* length scale. It is fundamentally because of these considerations that non-mean-field effects such as *intermediate phases* in glasses can be detected in Raman scattering.

Wavelengths of acoustic excitations such as longitudinal or transverse modes generally accessible in a typical BS setup are usually about 200 nm or longer. BS serves intrinsically as an extended length-scale or *mean-field probe* of vibrational excitations in glasses. The method is not expected to be sensitive to elements of medium range structures consisting of small rings (< 1.5 nm) wherein rigidity in disordered systems is nucleated. Thus, in sharp contrast to Raman scattering, Brillouin scattering is unlikely to detect the presence of non-mean-field effects such as *intermediate phases* in glasses.

BS measurements on binary Ge_xSe_{1-x} glasses at room temperature were performed over the $0.15 < x < 0.33$ composition range. In these measurements the scattering was excited using 647.1 nm excitation, and one observed the longitudinal acoustic (LA) mode near 20 Ghz. Since the exciting photon energy is somewhat less than the energy bandgaps of the glasses, the radiation penetrates the

samples and one probes bulk- rather than surface-effects. From a measurement of the LA mode frequency, refractive index and mass density, variations in the longitudinal elastic constant $C_{11}(x, Po)$ were established as a function of glass composition x and illumination power Po. The principal results appear in Fig. 9. At low power (Po = 2mW), one observes the intrinsic variation of $C_{11}(x)$ in the glasses. It consists of a nearly monotonic increase in C_{11} as a function of x or mean coordination number $\boldsymbol{r} = 2(1+x)$. Such a behavior was noted earlier in ultrasonic acoustic moduli measurements [53-56]. With increasing Po, a softening in C_{11} is manifested, amounting nearly to 50% near the critical composition, $x_c = 0.19(1)$, close to the mean-field rigidity transition $x_t = 0.20$ or $\boldsymbol{r_t} = 2.40$ in the present glasses. The *giant softening* as a function of Po near x_t is found to be reversible at Po < 7 mW. The softening of C_{11} due to an increase of sample temperature (thermal effects) was also independently established [52], along with sample temperature rise due to laser irradiation. These results have permitted separating thermal (< 10%) from athermal (> 90%) contributions to the observed softening. Fig. 9 displays the light-induced (athermal) component to the softening in C_{11}.

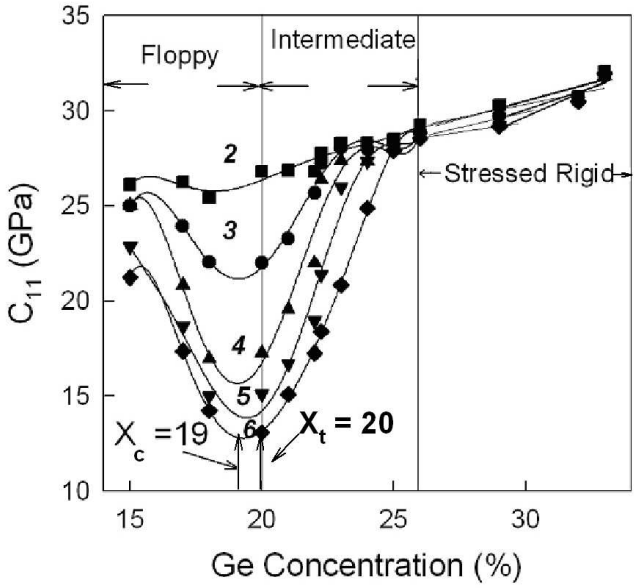

Fig. 9. Variations in longitudinal elastic constant, $C_{11}(x)$, in binary Ge_xSe_{1-x} glasses as a function of x from Brillouin scattering excited using 647.1 nm radiation. Each curve was obtained at a specific laser excitation power, Po in mW, indicated with each curve. Here r= 2(1+x), where x is expressed as a decimal fraction (see ref. [52]).

In these BS measurements the maximum in light-induced softening of C_{11} close to the mean-field rigidity transition highlights the importance of the backbone. A glass network near the rigidity transition is globally stress-free because it is optimally connected. These observations suggest that absence of

network stress near x = 0.19 serves to aid light-induced softening of glasses. Furthermore, the softening is centered near the *mean-field rigidity transition* because BS is intrinsically a *mean-field probe* of vibrational excitations in glasses.

Photo-structural transformations of Floppy and stressed-rigid networks

Glass compositions in intermediate phases are generally fully polymerized. Such is generally not the case in the stress-prone *floppy* and *stressed-rigid* glass compositions[24,25,57,58]. In chalcogenide glasses profound light-induced effects are observed in systems that are actually *partially polymerized* or *segregated on a nanoscale*. These trends are suggestive that in stress-prone networks light at low power is usually absorbed at free cluster surfaces, where bonding configurations can be altered without invoking large scale structural rearrangements of the backbone, and thus large cost in strain energies. We provide examples of both floppy and stressed-rigid systems where photo-polymerization of backbones is observed. In these Raman scattering experiments the exciting radiation serves both as a *pump* and also as a *probe* of light-induced effects.

Floppy networks (Ge-Se-I and Ge-S)

Melts of elemental Se can be readily cooled to form glasses that consist largely of polymeric Se_n chains. On the other hand, melts of elemental S upon cooling yield molecular crystals composed of S_8 crowns that can exist in two polymorphs. Addition of cross-linking cations such as Ge (or As) in binary alloy melts of $(Ge \text{ or } As)_x S_{1-x}$ composition will form glasses with varying concentrations of S_8 crowns present along with network forming $(Ge \text{ or } As)_t S_{1-t}$ backbones. Binary Ge_xS_{1-x} glasses at $x < 0.20$ represent examples of floppy glasses [33,59] that are segregated on a nanoscale having varying concentration of S_8 crown species. It is generally known that the concentration of S_8 monomers increases as the Ge concentration x of the binary glasses decreases. The S_8 ring concentration can be reliably ascertained in MDSC measurements[60] that show a polymerization transition [61], T_λ near a temperature of about 155º C. At $T > T_\lambda$, S_8 crowns first begin to open to form S_n chain-fragments leading to a pronounced increase of melt viscosities.

One may also track the presence of S_8 monomers and the backbone forming units in Raman scattering as is illustrated for a bulk glass sample of $Ge_{17}S_{83}$ composition in Fig. 10. Continued illumination of the glass sample with the 514.5 nm excitation leads to photo-structural changes that can be observed by recording Raman spectra of the glass sample after illumination for different time intervals of 5, 10, 15 and 20 minutes (Fig. 10). The evolution of lineshapes with illumination time shows that the scattering strength of the narrow S_8 mode near 219 cm^{-1} steadily decreases, while the frequency of the main A_1 band due to the symmetric stretch of corner-sharing GeS_4 terahedra systematically red-shifts. We have extracted the normalized scattering strength of the 219 cm^{-1} mode and

frequency of the A_1 mode by deconvoluting the Raman lineshapes and the results appear in Fig. 10b. These results show a linear correlation between the two observables at low integrated doses but the onset of a saturation as illumination times exceeds 15 minutes. These results have a rather straightforward interpretation.

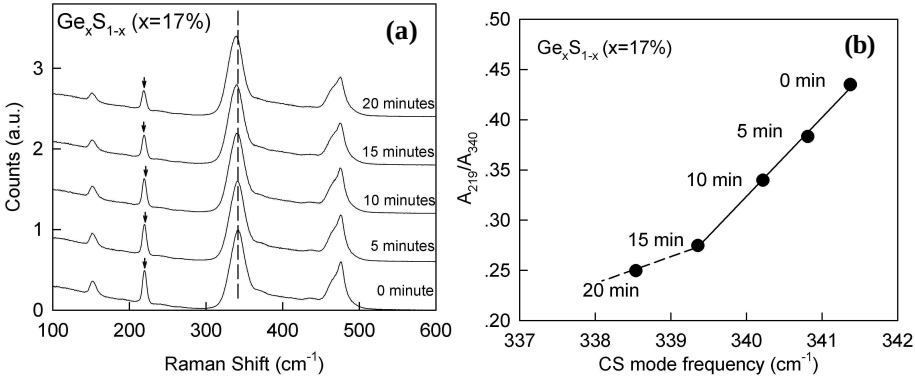

Fig. 10. (a) Raman scattering from bulk $Ge_{17}S_{83}$ glass excited using 514.5 nm radiation under micro Raman setup (3.05mW on sample) taken immediately after excitation (0 min), and after continuous irradiation for time intervals, t = 5, 10, 15 and 20 minutes as indicated on the observed lineshapes. (b)normalized scattering strength of the 219 cm^{-1} mode due to S_8 monomers plotted as a function of the mode frequency of the A_1 symmetric stretch of $Ge(S_{1/2})_4$ units near 340 cm^{-1}.

Progressive illumination of the virgin glass by band-gap radiation (514.5 nm) results in opening of S_8 monomers and the incorporation of S atoms in the backbone. The underlying photo-structural transformation drives the backbone to become S-richer than the starting glass composition. The photo-induced incorporation of S in the backbone decreases the global connectedness of the backbone, since it effectively lowers $x < 0.17$, and thus $\boldsymbol{r} = 2(1 + x)$. The optical signature of the underlying change is a *red-shift* of the A_1 mode near 340 cm^{-1}. The photo-alloying process can be visualized as the reverse of Ge chemical alloying in these glasses. In the later experiments a *blue-shift* of the A_1 mode was observed as global connectivity of the network was steadily increased by chemical alloying Ge. The later approach was used [33] when evidence for existence of the mean-field rigidity transition near $x = 0.23$ in binary Ge-S glasses was obtained from micro-Raman measurements.

Our second example of photo-structural transformations in a floppy glass system is that of the $Ge_{1/4}Se_{3/4-y}I_y$ ternary. In this chalcohalide glass system, we had noted earlier [23] that the intermediate phase resides in the $0.155 < y < 0.164$ iodine concentration range. The result suggests that glass compositions containing an excess of 16.4 molar percent of iodine are, in general, *floppy*. In such glasses, the backbone consists of mixed tetrahedral $Ge(Se_{1/2})_{4-m}I_m$ units having m = 0, 1, 2 and 3 iodine near neighbors with some but not all Se bridging across Ge atoms.

The m = 4 species, i.e., GeI_4, is a monomer and it decouples from the backbone. The narrow width of the vibrational mode near 155 cm^{-1} is the consequence of segregation of the m = 4 unit from the backbone.

Fig. 11 shows Raman scattering of a ternary glass at y = 0.324 excited using 647.1 nm radiation and a microscope attachment. Raman scattering permits tracking concentrations of mixed tetrahedral species through a measurement of their mode scattering strengths. The yellow-orange sample is transparent to the exciting radiation. Spectra were taken at different laser powers in the 1 < Po < 10 mW range, and evolution of lineshapes as a function of power established (Fig. 11). Vibrational modes of different m-species are identified and a rationale for the assignments is discussed elsewhere [23,40,62]. The central result of Fig. 11 is an increase in scattering strength of the m = 3, m = 2, and m = 1 species at the expense of the strength of the m = 4 and m = 0 species as the laser power is steadily increased from 1 to 10 mW. Table 1 gives a summary of the m-unit concentrations deduced from analysis of the observed Raman lineshapes. The observed results of Fig. 11 can be interpreted as follows. The underlying photo-polymerization process involves coalescing of m = 4 in the backbone (m = 0 units) to form m= 3 and m = 2 units by a pair of reactions,

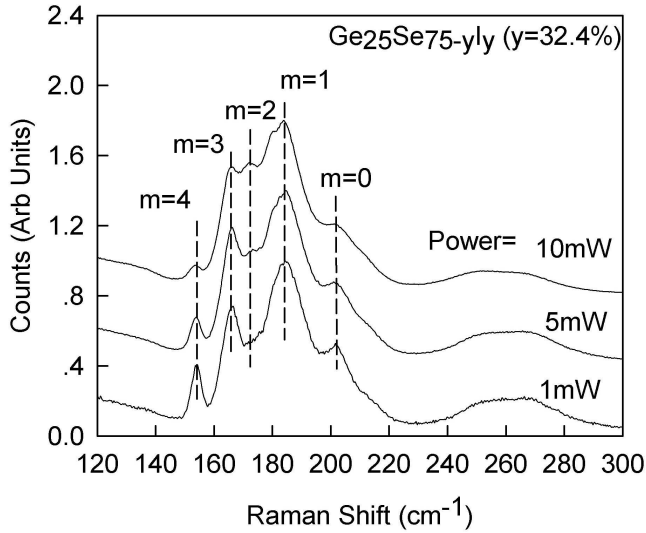

Fig. 11. Raman scattering in ternary $Ge_{1/4}Se_{3/4-y}I_y$ glasses excited using 647.1 nm line from a Kr^+ ion laser. An increase of laser power in the 1 < Po < 10 mW range leads to systematic lineshape changes that suggest photo-induced polymerization of the backbone. Upon removal of the pump radiation the backbone relaxes to its pristine state. In the micro-Raman setup, light is brought to a line focus on samples contained in evacuated quartz tubes. Thermal effects are expected to be minimal in such a set up. See ref.23 for details.

$$2\Delta N_4 + \Delta N_0 = 2\Delta N_3 + \Delta N_2 \qquad (3a)$$

$$\Delta N_3 + \Delta N_0 = \Delta N_2 + \Delta N_1 \quad (3b)$$

with a net result of,

$$2\Delta N_4 + 2\Delta N_0 = \Delta N_1 + 2\Delta N_2 + \Delta N_3 \quad (4)$$

In equation 3a, for example, ΔN_4 and ΔN_0 represent reduction in concentrations of N_4 and N_0 units brought about by the action of light as increases in N_3 units (ΔN_3) and N_2 units (ΔN_2) occur and form part of the backbone. In writing these reactions one conserves the number of iodine atoms on both sides of the equations. The first reaction is viewed as two monomeric m = 4 species converting to two m = 3 species by taking in two S atoms from an m = 0 species and giving two iodine atoms to transform an m = 0 species into an m = 2 species. The second reaction (3b) may be viewed as transforming a pair of m = 3 and m = 0 units into a pair of m = 2 and m = 1 units by exchanging an iodine atom. The concentrations of m-units deduced from our Raman results are shown in Table 1. No corrections for scattering cross-section of the modes were made in arriving at concentrations of the m-units given in Table 1. The simple model prediction here (equation 4) captures the essentials of the observed photo-structural transformations. The sign of the observed changes in concentrations of the different m-units is in harmony with the model. Quantitatively, the left hand side of equation 4 yields a net change in m-unit concentration of 0.10(2), while the right hand side yields a net change in m-unit concentrations of 0.05(1). The agreement between model prediction and our Raman scattering results is most encouraging given the simplicity of the model.

Table 1. Concentrations (N_m) of the m-species deduced from Raman spectra of Fig. 11 taken as a function of laser power. N_m represents the normalized concentration of respective m-units.

Power	**N_0**	**N_1**	**N_2**	**N_3**	**N_4**
1 mW	.14(1)	.47(1)	.024(10)	.25(1)	.12(1)
10 mW	.11(1)	.50(1)	.029(10)	.26(1)	.10(1)

The results described above on two *floppy* glass systems carry a central message; illumination with near-bandgap radiation leads to photo-polymerization of backbones. In these Raman scattering experiments the light-induced effects are *reversible*, i.e., removal of pump radiation eventually relaxes back the network to its partially polymerized pristine state. Furthermore, in these Raman scattering measurements irradiation of glass samples was performed in a controlled environment to avoid surface oxidation effects. These results are quite different in character from those reported on vapor deposited amorphous thin-films of chalcogenide systems wherein nanoscale segregation frozen by virtue of synthesis is *irreversibly* changed [63] by the action of light. And in some instances surface

oxidation effects on thin-films [64] have intrinsically contributed to promoting photo-structural transformations as samples are exposed at ambient conditions.

Stressed rigid networks

Stoichiometric $GeSe_2$ glass is a model example of a *stressed-rigid* glass with a mean coordination number of $\boldsymbol{r} = 2.67$. Molecular structure of the bulk glass has been extensively examined in neutron scattering [65], Raman scattering [51,58,66,67], ab-initio molecular dynamic simulations[68,69], and Mossbauer spectroscopy[58,69]. Convincing evidence for existence of a small but finite concentration of homopolar bonds in the stoichiometric material has accumulated from a number of methods [51,58,65-71]. In Raman scattering, for example, a mode near 180 cm^{-1} is identified with presence of Ge-Ge bonds [51,58, 67]. Such bonds first appear near a glass composition, $x = 0.31$ in binary Ge_xSe_{1-x} glasses, a composition where the slope of T_g with x shows a global maximum [58]. The later observation is not an accident, but constitutes evidence for the fact that Ge-Ge bonds once formed in this binary glass system lower the global connectivity of the backbone. Apparently these bonds must not form part of the backbone but actually segregate on a nanoscale. The *stressed-rigid* glass is, thus, an example of a mildly depolymerized network. In the early 1980s, Griffiths et al.[72] studied Raman scattering from the stoichiometric glass as a function of increasing laser power, and were able to observe *reversible micro-crystallization* as sketched in the results of Fig. 12 taken from their work. In these experiments, a $GeSe_2$ bulk glass was cooled to 78K in a cryostat and illuminated by 647 nm radiation from a Kr^+ ion laser serving to pump as well as probe the photo-structural transformations [72]. The results of Fig. 12 show that upon increasing the Kr laser power from 24 mW (lineshape A) to 50 mW (lineshape B) to 84 mW (lineshape C) , one observes, (i) the mode at 180 cm^{-1} to completely vanish, (ii) the A_1 mode to narrow and blue-shift from 200 cm^{-1} to 210 cm^{-1} and (iii) inter-layer lattices modes in the $0 < \nu < 120$ cm^{-1} range to emerge. All these observations (i-iii) are consistent with the partially polymerized backbone reconstructing with a second nanophase (containing Ge-Ge bonds) to fully polymerize, and then microcrystallize. In these investigations the sample was held at 78 K, underscoring that structural changes are optically- and not thermally-driven. The underlying photo-structural transformations are *reversible* in character because upon reducing the power to 20 mW (lineshape D), nearly half of the microcrystallized sample reverted to the glass phase as the pump power was reduced by a factor of 4. At this stage, the sample was allowed to relax at an elevated temperature (300K) for 45 min. with minor changes (lineshape E). However, a complete recovery to the virgin glass state (lineshape F) occurred after the sample was allowed to relax for a longer period (17 hours) at 300 K.

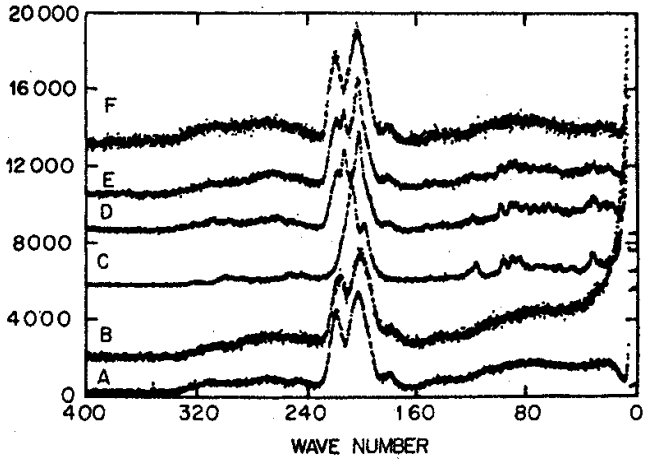

Fig. 12. Photostructural transformation in $GeSe_2$ glass showing reversible microcrystallization monitored in Raman scattering. Fig. is taken from ref. 72.

In summary, $GeSe_2$ glass represents an example a *stressed rigid* network possessing a molecular structure that is almost *fully* polymerized. Illumination by near bandgap radiation leads to photo-structural transformations as a function of increasing laser power, and includes internal surface reconstruction of the Se-rich $GeSe_{2+\xi}$ backbone with a Ge-rich nano-phase (containing Ge-Ge bonds) to result in a *fully polymerized* network that can be microcrystallized and which can revert back to the virgin glass state upon removal of the photon pump. GeS_2 glass is another example of a stressed-rigid network whose chemical order is intrinsically broken [73] due to incomplete polymerization of the backbone [57]. Pressure induced polymerization of the GeS_2 backbone has also been observed [74] in Raman scattering measurements performed using Diamond Anvil Cells.

Photo-darkening and network connectedness

Since the pioneering work of Ka. Tanaka [1], a vast literature on the phenomenon of photo-darkening of chalcogenide glasses and thin-films has evolved [12, 13]. The subject was recently reviewed by H. Fritzsche [12]. The narrowing of optical gap (ΔE) is pronounced [75] in Sulfides, lower in Selenides and least in Telluride glasses (Fig. 13). The athermal nature of the effect is clear from enhancement of ΔE at low temperatures ($T < T_g$). And it is most fortunate that such experiments were reported [76] on *thin polished platelets* of bulk Ge_xSe_{1-x} glasses in the early 1980s, long before the intermediate phase was discovered. The results of Fig. 14 are taken from the work of S. Mamedov et al. [76], who cleverly tuned sample thicknesses to have the *same starting value of transmission* at different x for the 633 nm radiation used in the photodarkening measurements. The advantage of using bulk glasses over vapor deposited thin-films cannot be over-

emphasized. One can control chemical composition and homogeneity, and molecular structure in bulk glasses much better than in vapor deposited thin-films [77]. The bulk glass results show photo-darkening to have a global maximum [76] near x = 0.25. The maximum in photodarkening overlaps with the *intermediate phase* in binary Ge_xSe_{1-x} glasses rather well. Although results on annealed thin-films [76] are sparse, the observed trends in photodarkening in films studied by Mamedov et al. are certainly consistent with their results on bulk glasses.

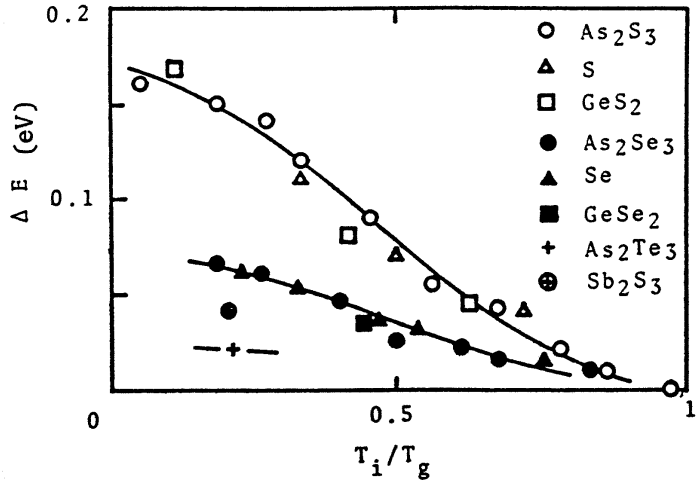

Fig. 13. Reduction in optical gap (ΔE) upon illumination with near band-gap radiation at a temperature T_i normalized to T_g in glasses based on sulfides, selenides and tellurides. Fig is taken from ref. 75.

The maximum in photodarkening in the *intermediate phase* of Ge-Se glasses is expected. It highlights the very special role of host network *elastic response* in optimizing the athermal response. Intermediate phases are optimally constrained phases in which light-induced switching of covalent bonds can globally propagate, and a dynamic equilibrium between incident light energy and photoelastic response of a network as a whole can occur. The absence of network stress in intermediate phases lowers energy barriers for local bond rearrangements to occur, and the backbone as a whole can soften (photo-diffusion) in initial stages, and melt (photomelting) at higher illumination flux. The absence of network stress facilitates light-induced local- and global- chemical bond rearrangements that lead not only to photo-darkening but also to photo-expansion as has been widely observed. In *floppy* and *stressed-rigid* elastic phases of the Ge-Se glasses photo-darkening is qualitatively suppressed because light-induced structural rearrangements are largely localized where light is absorbed. In such networks, energy barriers to bond switching are much larger because of the intrinsically higher stresses in these selenide glasses that are generally better polymerized than their sulfide analogues. The light-soaked state of an optimally constrained glass network is a dynamic *random network state* lacking the medium range structure that prevailed in the virgin *self- organized state*.

Recently, first-principles electronic structure calculations [14,78] on a suitably terminated $AsSH_3$ cluster have been performed to understand the origin of photodarkening in As_2S_3. In these self-consistent field Hartree-Fock calculations total energies of the electronic ground state and first excited are evaluated as a function of the S bridging angle. The results reveal [14] opening of the bridging As-S-As angle in the singlet excited state in relation to the ground state by about 7° that leads to a narrowing of the gap by 0.35(20) eV. The opening of the S-bridging angle upon excitation is confirmed from EXAFS experiments of Lee et al.[79]. The calculated optical edge shift is in harmony with the observations. Parallel calculations [14] on GeS_2 lead, however, to a shift of 0.73(30) eV that is larger than the observed results. And as recognized by Lucovsky [14], the calculations work well for As_2S_3 glass and fail for GeS_2 glass because in the latter substantial network stress must occur. Such cluster calculations, understandably, are unable to fold in the elastic response of a host network [14, 80]. The importance of *intermediate phases* in design of the new high k thin-film gate dielectrics for the next generation of microelectronic devices has emerged in recent years by the pioneering efforts of G. Lucovsky [81]. Here we have attempted to highlight the importance of *intermediate phases* to understanding photo-structural transformations in glasses.

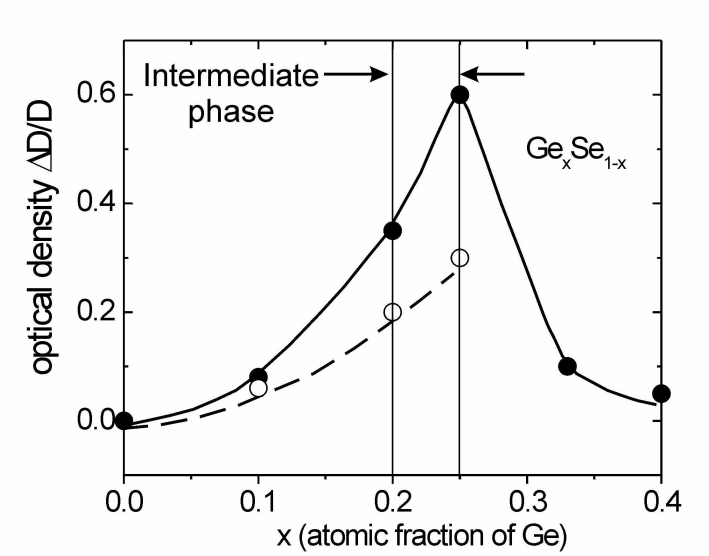

Fig. 14. Photo-darkening as reflected in changes of optical density (ΔD/D) in glass platelets (●) and annealed thin-films (○) in the Ge_xSe_{1-x} binary reported by S. Mamedov et al. ref . [76]. Note the maximum in photo-darkening near x = 0.25 overlaps with the intermediate phase.

Concluding remarks

In this review we have collected select Raman scattering and Brillouin scattering measurements on chalcogenide glasses that highlight the role of *network*

connectedness on understanding *light-induced effects* in glasses and amorphous thin-films. There are many other experiments that have a close bearing to the issue at hand, and we mention some of these in passing. In a series of measurements on obliquely deposited chalcogenide thin-films, K. L. Chopra and collaborators [3,82, 83] discovered giant photo-contraction effects (~ 20%) in the Ge-Se binary possessing a mean-coordination number ***r*** of 2.50. Although presence of columnar structures in obliquely deposited thin-films is not peculiar to chalcogenide based materials, the light-induced densification of such films certainly is. These observations can also be understood as a direct consequence of photo-melting of the intermediate phase in the Ge-Se and Ge-As-Se systems.

Opto-mechanical effects observed in cantilevers made of binary As_xSe_{1-x} thin-films are more pronounced in As-rich compositions near x = 0.50 and 0.57 than at the stoichiometric composition x = 0.40 as suggested by the work of S. R. Elliot and collaborators [5]. The *intermediate phase* in the As-Se binary resides in the $0.29 < x < 0.37$ range [32]. Stressed-rigid glasses at $x > 0.45$ become progressively de-mixed as As_4Se_4 monomers begin to decouple from the As-rich backbone. The experimental evidence comes independently from T-modulated DSC [32] and Raman scattering [85]. T_gs of the glasses begin to decrease once $x > 0.40$ suggesting that in As-rich glasses the group V additive segregates from the backbone on a nanoscale. Furthermore, the non-reversing enthalpy in such glasses instead of progressively increasing with x, begins to decrease once $x > 0.50$ to almost vanish near x = 0.60, again pointing to a rapid loss of the connective backbone tissue. Inelastic neutron scattering [84] on a glass at x = 0.60 establishes this composition to be an exception to the vibration iso-coordination rule, reinforcing the low effective connectivity of the backbone due to de-mixing. The view is corroborated from FT- Raman studies that show evolution of sharp modes on the main vibrational band centered near 250 cm^{-1} in the As-rich glasses ($x > 0.45$), arising from the presence of clusters [85]. Near band-gap radiation serves to fuse internal surfaces of the fragmented $As_{0.50}Se_{0.50}$ backbone with increasing illumination power to elongate films and build tensile stresses. The light polarization sensitive nature of the mechanical transformation may aid understanding how the As-rich clusters reversibly open to become part of the backbone and close to decouple from it [5].

The celebrated case of As_2S_3 glass flakes displaying pronounced low temperature photo-expansion [2] is a particularly interesting system. As_2S_3 glass appears to be an example of a *mildly stressed rigid* network [86] in which some de-mixing on a nanoscale appears to be an intrinsic feature of the stoichiometric bulk glass [26]. The thermally reversing window in the As_xS_{1-x} binary is observed [86] in the $0.20 < x < 0.27$ range, and excludes the stoichiometric glass composition ($x = 2/5$). It is likely that de-mixing of the stoichiometric glass actually *assists* photo-expansion for reasons discussed above in the case of AsSe. The view is corroborated by recent observations [87, 88] of changes in Raman depolarization of As_2S_3 fibers as a function of tensile stress. The absence of such changes in the S-richer composition, $As_{27}S_{73}$, a composition that lies close to the intermediate phase [86] and is thought to be fully polymerized, reinforces the view that photomelting effects in As_2S_3 glass are largely promoted because of its de-mixed character.

The conclusions from the present chapter can be summarized as follows. Illumination of glasses and amorphous thin-films by pair-producing radiation

results in local structural rearrangements due to the metastability associated with lone-pair states on chalcogens. Such rearrangements propagate globally in networks that are stress-free as in *intermediate phases*. A pristine *self-organized state* is dynamically transformed into a light-soaked *random network state* leading to pronounced photo-diffusion, photo-expansion and eventually photo-melting. On the other hand, such local structural changes do not propagate globally in stress-prone networks as in *floppy* and *stressed-rigid* elastic phases. In the later phases, glasses and amorphous films in their virgin state are usually found to be *de-mixed* (segregated on a nanoscale), and photo-polymerization effects abound as free internal surfaces reconstruct leading amongst other things to photo-elongation effects.

Acknowledgements

It is a pleasure to acknowledge discussions with G. Lucovsky, B. Goodman, S. Mamedov, R. Sooryakumar, D. McDaniel, Tao Qu, and Daniel Georgiev. This work is supported by NSF grant DMR 01-01808.

References

[1] Ka. Tanaka, Structure and Excitations in Amorphous solids, Edited by G. Lucovsky, F. L. Galeener (American Institute of Physics, New York, 1976) p.148.
[2] H. Hisakuni, K. Tanaka, Science **270**, 974 (1995).
[3] K. L. Chopra, K. S. Harshvardhan, S. Rajgopalan, L. K. Malhotra, Solid State Commun. **40**, 387 (1981); P. Boolchand, W. J. Bresser, K. L. Chopra, Bull. Am. Phys. Soc. **44**, 1434 (1999).
[4] T. Wagner, M. Frumar, Photo-induced Metastability in Amorphous Semiconductors, Edited by A. V. Kolobov (Wiley-VCH GmbH and Co, KGaA,2003) p.160 and references therein.
[5] P. Krecmer, A. M. Moulin, R. J. Stephenson, T. Rayment, M. E. Well, S. R. Elliott, Science **277**, 1799 (1997).
[6] V. V. Poberchii, A. Kolobov, K. Tanaka, Appl. Phys. Letters **72**, 1167 (1998).
[7] V. Lyubin, M. Klebanov, M. Mitkova, T. Petkova, J. Non Cryst. Solids **227**, 739 (1998).
[8] M. N. Kozicki, W. C. West, Programmable Metallization Cell, U.S. Patent **5**, 896, 312(1999).
[9] T. Ohta, J. Optoelectron. Adv. Mater.**3**, 609 (2001). Also see T.Ohta and S. R. Ovshinsky in Photo-induced Metastability in Amorphous Semiconductors, edited by A. V. Kolobov (Wiley-VCH GmbH and Co, KGaA,2003) p.310.
[10] J. Mort, The Anatomy of Xerography (McFirland and Co, London, UK, 1989).
[11] S. O Kasap, J. A. Rowlands, in Insulating and Semiconducting Glasses, Edited by P. Boolchand, (World Scientific Press, Inc., Singapore, 2000), p.781.

[12] H. Fritzsche, Solid State Commun. **99**, 153 (1996). For a recent review, see H. Fritzsche in Insulating and Semiconducting Glasses, Ed. P. Boolchand, (World Scientific Press, 2000), p. 653.
[13] K. Shimakawa, A. Kolobov, S. R. Elliott, Advances in Physics **44**, 475 (1995). Also see K. Shimakawa and A. Ganjoo, J. Optoelectron. Adv. Mater. **3**, 167(2001).
[14] T. Mower, G. Lucovsky, L. S. Sremaniak, J. L. Whitten J. Non-Cryst. Solids (in press).
[15] K. Shimakawa, N. Yoshida, A. Ganjoo, A. Kuzunawa, J. Singh, Phil. Mag. Lett. **77**, 153 (1998).
[16] P. Boolchand, D. G. Georgiev, B. Goodman, J. Optoelectron. Adv. Mater. **3**, 703 (2001).
[17] J. C. Phillips, Phys. Rev. Lett. **88**, 216401 (2002).
[18] M. F. Thorpe, D. J. Jacobs, M. V. Chubynsky, J. C. Phillips, J. Non-Cryst. Solids **266-269**, 859 (2000).
[19] P. Boolchand, D. G. Georgiev, M. Micoulaut, J. Optoelectron. Adv. Mater. **4**, 823 (2002).
[20] Tao Qu, B. Goodman, P. Boolchand (unpublished). Tao Qu Ph.D. Dissertation (2004), University of Cincinnati, (unpublished).
[21] S. Chakravarty, D. G. Georgiev, P. Boolchand, M. Micoulaut (unpublished). Cond- mat/0308016
[22] P. Boolchand, X. Feng, W. J. Bresser, J. Non Cryst. Solids **293-295**, 348 (2001).
[23] Fei Wang, M. S. Thesis (2003), University of Cincinnati, (unpublished), Ph.D. Thesis (2004), University of Cincinnati, (unpublished).
[24] P. Boolchand, D. G. Georgiev, T. Qu, F. Wang, L. Cai, S. Chakravarty, CR Chimie **5**, 713 (2002).
[25] S. Mamedov, D. G. Georgiev, Tao Qu, P. Boolchand. J. Physics: Cond. Matter. **15**, S2397 (2003).
[26] D. G. Georgiev, P. Boolchand, K. A. Jackson. Phil. Mag. **83**, 2941 (2003).
[27] D. G. Georgiev, P. Boolchand, H. Eckert, M. Micoulaut, K. Jackson, Europhysics Lett. **62**, 49 (2003).
[28] J. C. Phillips, J. Non Cryst. Solids **34**, 153 (1979).
[29] M. F. Thorpe, J. Non-Cryst. Solids **57**, 355 (1983).
[30] J. C. Phillips in Rigidity Theory and Applications, Edited by M.F.Thorpe and P. M. Duxbury, (Kluwer Academic/Plenum Publishers, New York, 1999) p. 155. Also see M. F Thorpe, ibid. p. 239.
[31] D. Selvanathan, W. J. Bresser, P. Boolchand, Phys. Rev. B **61**, 15061 (2000).
[32] D. G. Georgiev, P. Boolchand, M. Micoulaut, Phys. Rev B **62**, R9228 (2000).
[33] Xingwei Feng, W. J. Bresser, P. Boolchand, Phys. Rev. Lett. **78**, 4422 (1997).
[34] Tao Qu, D. G. Georgiev, P. Boolchand, M. Micoulaut in Supercooled Liquids, Glass Transition and Bulk Metallic Glasses, edited by T. Egami, A. L. Greer, A. Inoue and S. Ranganathan (Materials. Research Society, PA) p.111.
[35] S. Chakravarty, P. Boolchand (unpublished). S. Chakravarty, M. S. Dissertation (2003), University of Cincinnati, (unpublished).
[36] M. Micoulaut, J. C. Phillips Phys. Rev. B **67**, 104204 (2003).
[37] Y. Wang, P. Boolchand, M. Micoulaut, Europhys. Lett. **52**, 633 (2000).

[38] A. Feltz, H. Aust, A. Blayer, Journal of Non-crystalline Solids **55**, 179-190 (1983).
[39] M. F. Thorpe, N. V. Chubynsky in Phase Transitions and Self-Organization in Electronic and Molecular Networks, Edited by J. C. Phillips and M. F. Thorpe, (Kluwer Academic/Plenum Publishers, New York, 2001) p.43.
[40] Fei Wang, P. Boolchand, K. Jackson, Proceedings of Non-Crystalline Materials Conference 9 (to appear).
[41] R. Kerner, M. Micoulaut, Journal of Non-Cryst. Solids **210,** 298 (1997).
[42] M. Micoulaut, The Eur. Phys. Journal **1B,** 277 (1998).
[43] H. He, M. F. Thorpe, Phys. Rev. Lett. **54**, 2107 (1985).
[44] D. S. Franzblau, J. Tersoff, Phys. Rev. Lett. **68**, 2172 (1992).
[45] Y. Wang, J. Wells, D. G. Georgiev, P. Boolchand, K. Jackson, M. Micoulaut, Phys. Rev. Lett. **87**, 185503 (2001).
[46] P. Boolchand, M. F. Thorpe. Phys. Rev. B **50**, 10366 (1994).
[47] M. Mitkova, P. Boolchand, Journal of Non-Crystalline Solids **240**, 1(1998).
[48] B. A. Weinstein, R. Zallen, in Light Scattering in Solids I", Edited by M. Cardona and G. Guntherodt (Springer, Berlin, 1984), p. 463.
[49] T. Chattopadhyay, C. Carlone, A. Jayaraman, H. G. v. Schnering,
. Phys. Rev B **23**, 2471 (1981).
[50] K. Murase, T. Fukunaga, Optical Effects in Amorphous Semiconductors, Edited by P. C. Taylor and S. G. Bishop, (American Institute of Physics, New York,1984) p. 499.
[51] K. Murase, in Insulating and Semiconducting Glasses, Edited by P. Boolchand (World Scientific Press Inc., Singapore, 2000), p. 415.
[52] J. Gump, I. Finkler, H. Xia, R. Sooryakumar, W. J. Bresser, P. Boolchand, Phys. Rev. Lett. (in press).
[53] S. S. Yun, Hui Li, R. L. Cappelletti, R. N. Enzweiler, P. Boolchand, Phys. Rev. B **39**, 8702 (1989).
[54] J. Y. Duquesne, J. Bellessa, J. Phys. (Paris) Colloq. **46**, C10-445 (1985).
[55] R. Ota, T. Yamate, N. Soga, M. Kumugi, J. Non Cryst. Solids **29**, 67 (1978).
[56] B. L. Halfpap, S. M. Lindsay, Phys. Rev. Lett. **57**, 847(1986).
[57] L. Cai, P. Boolchand. Phil. Mag. B **82**, 1649 (2002).
[58] P. Boolchand, W. J. Bresser, Phil. Mag. B **80**, 1757 (2000).
[59] T. Wagner, S. O. Wagner, M. Vlcek, A Sklenar, A. Stronski, J. Materials Science **33**, 5581 (1998).
[60] Tao Qu, P. Boolchand, cond-mat/0312481.
[61] A. T. Ward, Advances in Chemistry Series **110**, 163 (1971).
[62] K. Jackson, A. Briley, S. Grossman, D. V. Porezag, M. R. Pederson, Phys. Rev. B **60**, R14985 (2001).
[63] K. Antoine, J. Li, D. A. Drabold, H. Jain, M. Vlcek, A. C. Miller, J. Non Cryst. Solids, 326 & 327, 248 (2003).
[64] G. Chen, H. Jain, M. Vlcek, S. Khalid, J. Li, D. Drabold, S. Elliott, Appl. Phys. Letters **82**, 706 (2003).
[65] P. S. Salmon, I. Petri, J. Phys. Condens. Matter **15**, S1509 (2003).
[66] S. Sugai, Phys. Rev. B **35**, 345 (1987).
[67] Y. Wang, T. Nakaoka, K. Murase, in Phase Transitions and Self-Organization in Electronic and Molecular Networks, Edited by J. C. Phillips and M. F. Thorpe, (Kluwer academic/ Plenum Publishers, 2001), p.85.

[68] C. Massobrio, A. Pasquerello, R. Car, Phys. Rev B **64**, 144205(2001).
[69] D. Drabold, J. Li, D. N. Tafen, J. Phys. Condens. Matter **15**, S1529 (2003).
[70] P. Boolchand, J. Grothaus, J. C. Phillips, Solid State Commun. **45**, 183 (1983).
[71] I. Petri, P. S. Salmon, H. E. Fischer, Phys. Rev. Lett. **84**, 2413 (2000).
[72] J. E. Griffiths, G. P. Espinosa, J. P. Remeika, J. C. Phillips, Phys. Rev. B**25**, 1272 (1982).
[73] S. Blaineau, P. Jund, D. A. Drabold, Phys. Rev. B **67**, 094204 (2003).
[74] B. A. Weinstein an M. L. Slade in Optical Effects in Amorphous Semiconductors edited by P .C. Taylor and S.G. Bishop (American Institute of Physics, New York,1984) p. 457.
[75] Ke. Tanaka, J. Non Cryst. Solids **59-60**, 925 (1983).
[76] S. B. Mamedov, M. D. Mikhailov, I. M. Pecheritsyn, Fiz. Khim. Stekla, **7**(4), 503 (1981).
[77] P. Nagels, R. Mertens, L. Tichy, in Properties and Applications of Amorphous Materials, Edited by M. F. Thorpe and L. Tichý, Kluwer Academic Publishers, Boston, 2001), p.25.
[78] J. L. Whitten, Y. Zhang, M. Menon, G. Lucovsky, J. Vac. Sci. Technol. B **20**, 1710 (2002).
[79] J. M. Lee, M. A. Paesler, D. E. Sayers, Journal of Non-crystalline Solids **123**, 295-309 (1990)
[80] T. Uchino, D. C. Clary, S. R. Elliott Phys. Rev. Lett. **85**, 3305 (2000).
[81] G. Lucovsky, H. Yang, H. Niimi, J. W. Keister, J. E. Rowe, M. F. Thorpe, J. C. Phillips, J. Vac. Sci. Technol. B **18**, 1742 (2000).
[82] B. Singh, S. Rajagopalan, P. K. Bhat, D. K. Pandya, K .L. Chopra, Solid State Commun. **29**, 167 (1979).
[83] B. Singh, S. Rajagopalan, P. K. Bhat, D. K. Pandya, K. L. Chopra, J. Non Cryst. Solids, **35&36**, 1053 (1980).
[84] B. Effey, R. L. Cappelletti, Phys. Rev B **59**, 4119 (1999).
[85] M. Frumar, B. Frumarova, T. Wagner, P. Nemec, in Photo-Induced Metastability in Amorphous Semiconductors, Edited by A. V. Kolobov, (Wiley-VCH,Verlag and Co KGaA, 2003) p.24.
[86] D. G. Georgiev, Ph. D. Dissertation (2003), University of Cincinnati, unpublished.
[87] S. N. Yannopoulos in Photo-Induced Metastability in Amorphous Semiconductors, edited by A. V. Kolobov (Wiley-VCH Verlag & Co.KGaA, 2003) p. 119 and references therein.
[88] D. Th. Kastrissios, G. N. Papatheodorou, S. N. Yannopoulos, Phys. Rev. B **64**, 214203 (2001).